iScience, Volume *24*

Supplemental information

Polyclonal F(ab')$_2$ fragments of equine antibodies raised against the spike protein neutralize SARS-CoV-2 variants with high potency

Luis Eduardo R. Cunha, Adilson A. Stolet, Marcelo A. Strauch, Victor A.R. Pereira, Carlos H. Dumard, Andre M.O. Gomes, Fábio L. Monteiro, Luiza M. Higa, Patrícia N.C. Souza, Juliana G. Fonseca, Francisco E. Pontes, Leonardo G.R. Meirelles, José W.M. Albuquerque, Carolina Q. Sacramento, Natalia Fintelman-Rodrigues, Tulio M. Lima, Renata G.F. Alvim, Federico F. Marsili, Marcella Moreira Caldeira, Russolina B. Zingali, Guilherme A.P. de Oliveira, Thiago M.L. Souza, Alexandre S. Silva, Rodrigo Muller, Daniela del Rosário Flores Rodrigues, Luciana Jesus da Costa, Arthur Daniel R. Alves, Marcelo Alves Pinto, Andréa C. Oliveira, Herbert L.M. Guedes, Amilcar Tanuri, Leda R. Castilho, and Jerson L. Silva

SUPPLEMENTAL INFORMATION

Polyclonal F(ab')$_2$ fragments of equine antibodies raised against recombinant SARS-CoV-2 spike protein neutralize the P.1 and P.2 strains with high potency

Luis Eduardo R. Cunha[1]*, Adilson A. Stolet[1]*, Marcelo A. Strauch[1]*, Victor A. R. Pereira[2,3]*, Carlos H. Dumard[2,3]*, Andre M. O. Gomes[2,3]*, Fábio L. Monteiro[4]*, Luiza M. Higa[4]*, Patrícia N. C. Souza[1], Juliana G. Fonseca[1], Francisco E. Pontes[1], Leonardo G. R. Meirelles[1], José W. M. Albuquerque[1], Carolina Q. Sacramento[5,6], Natalia Fintelman-Rodrigues[5,6], Tulio M. Lima[7], Renata G. F. Alvim[7], Federico F. Marsili[7], Marcella Moreira Caldeira[2,3], Russolina B. Zingali[2,3], Guilherme A. P. de Oliveira[2,3], Thiago M. L. Souza[5,6], Alexandre S. Silva[8], Rodrigo Muller[9], Daniela del Rosário Flores Rodrigues[8], Luciana Jesus da Costa[10], Arthur Daniel R. Alves[8], Marcelo Alves Pinto[7], Andréa C. Oliveira[2,3], Herbert L. M. Guedes[11,,12,13], Amilcar Tanuri[3,4#], Leda R. Castilho[7#], Jerson L. Silva[2,3#]

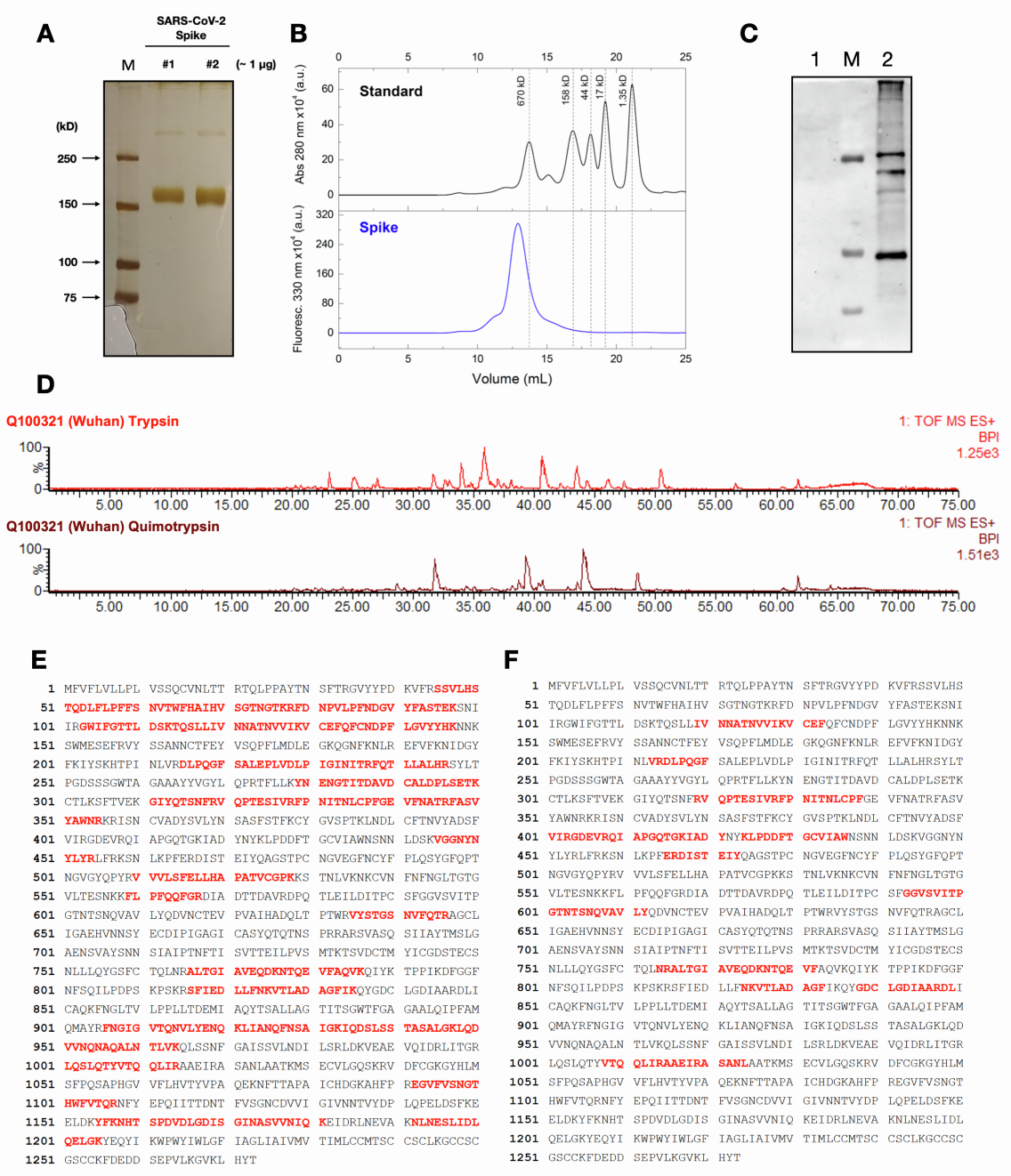

Figure S1. Quality checks of SARS-CoV-2 spike protein (related to Figure 1). **(A)** Image of a silver-stained 7% SDS-PAGE gel showing two representative batches of SARS-CoV-2 spike preparation (two batches for purposes of comparison). **(B)** Line plots showing size-exclusion chromatograms using a Superose 6 10/300 column. The fluorescence intensity at 330 nm of the spike protein was recorded as a function of the retention volume. The absorbance at 280 nm of a molecular mass standard (black line) is shown for comparison. **(C)** Western-blot membrane for detection of host-cell proteins (HCP) from HEK293 cells using a specific antibody (#ABIN1113182, Antibodies-Online.com, 1:1.000). Lane 1, Purified SARS-CoV-2 spike preparation (15 µL of sample, containing 13 µg of protein, was applied to the gel); Lane 2, Molecular-mass marker (Bio-Rad,

#1610374); Lane 3 supernatant of HEK293 cells as positive control for HCP (15 μL of sample was applied to the gel). **(D)** Ion counts as a function of elution time of tryptic (red) and quimotryptic (dark red) peptides from a C18 column. Mapping of (E) tryptic and (F) quimotryptic peptides against the SARS-CoV-2 spike sequence comprises a total coverage of ca. 44%.

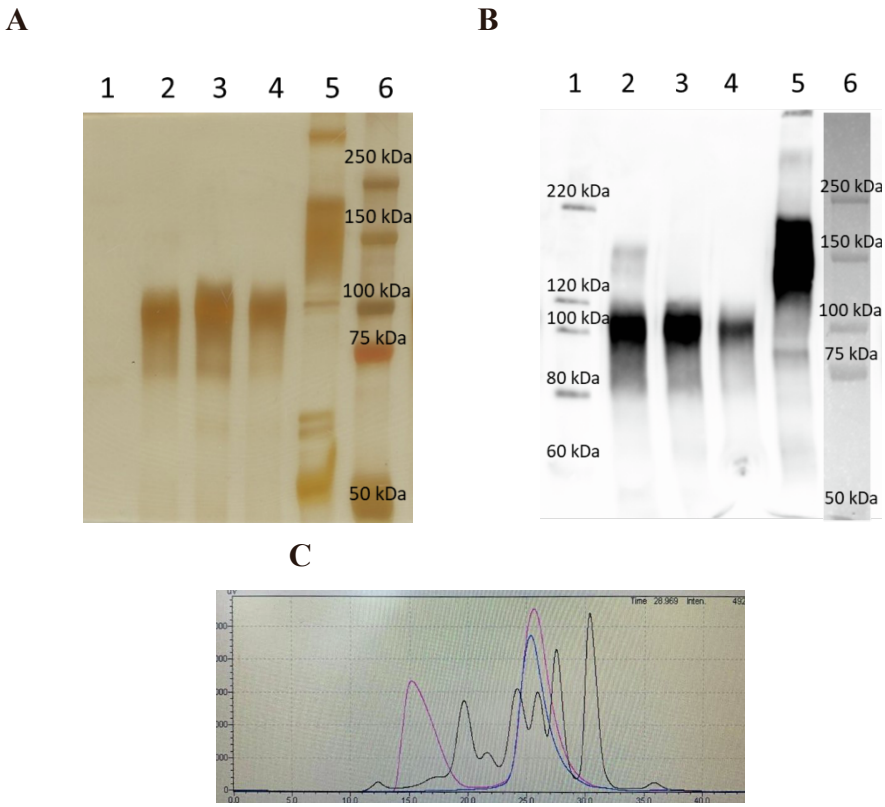

Figure S2. Silver-stained SDS-PAGE (A), chemiluminescent Western blot (B) and Gel Filtration of equine hyperimmune F(ab')$_2$ anti-SARS-CoV-2 (related to Figures 3C and 4). A, B: 1. MagicMark XP MW Markers (Thermo Fisher); 2. Concentrated hyperimmune anti-SARS-CoV-2 F(ab')$_2$ (1:200); 3. Ampouled antivenom F(ab')$_2$ (1:200); 4. Ampouled anti-rabies F(ab')$_2$ (1:200); 5. Equine hyperimmune plasma (1:200); 6. Precision Plus Protein Dual Color Markers (Bio-Rad). **C:** Size-exclusion chromatograms using a Superose 6 10/300 column. Blue line: Industrial concentrated hyperimmune anti-SARS-CoV-2 F(ab')$_2$; Rose Line: Pre-industrial lot of anti-SARS-CoV-2 F(ab')$_2$; Black line: Molecular markers.

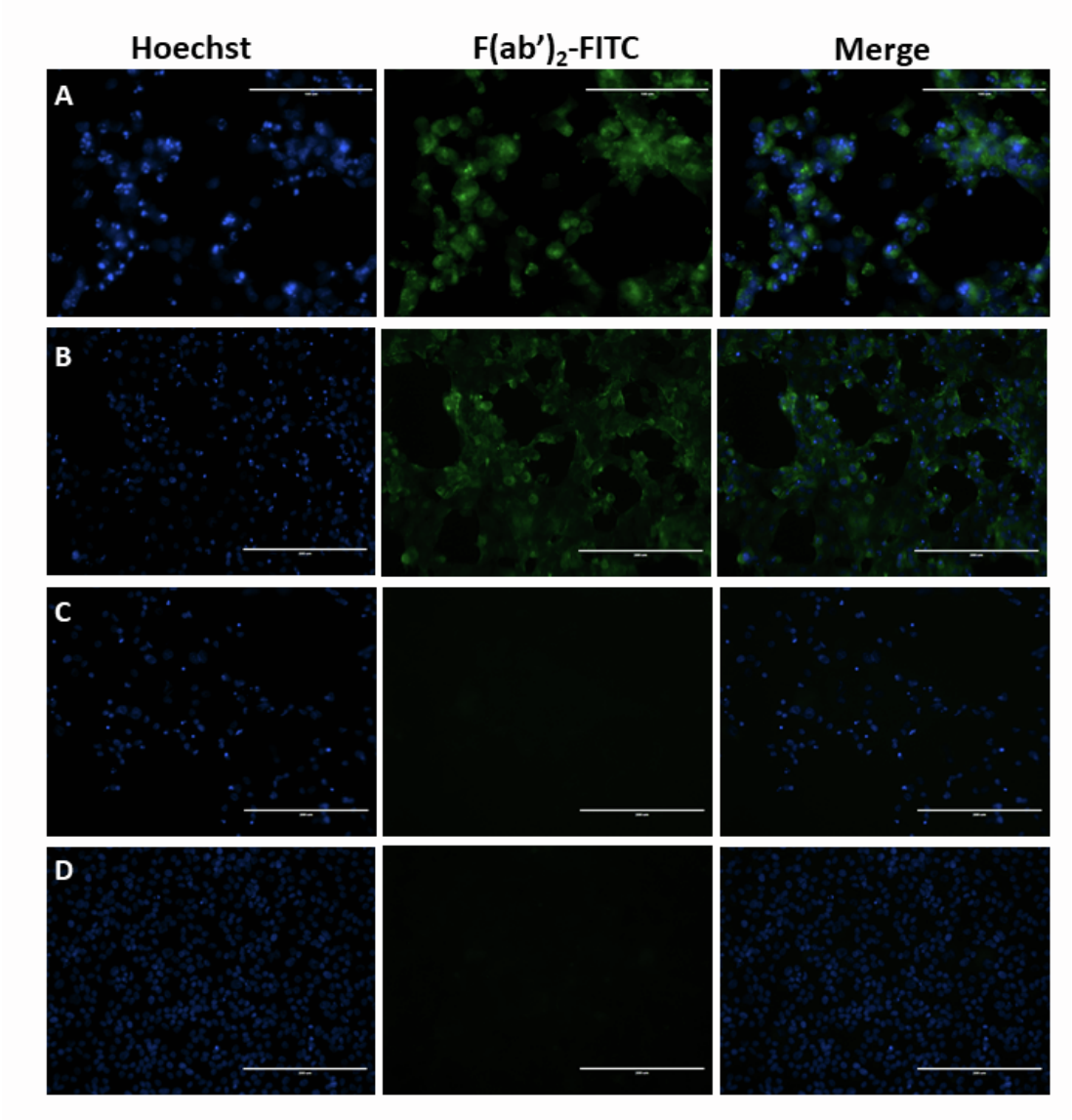

Figure S3: Equine F(ab')$_2$ binds specifically to SARS-CoV-2 infected cell (related to Figures 3C and 4). Vero E6 cells were infected with SARS-CoV-2 (MOI = 0.05) for 48 h and immunolabeled with F(ab')$_2$-FITC conjugate. **(A)** Cells infected with SARS-CoV-2, labeled with F(ab')$_2$ -FITC, and observed with 40x objective. **(B)** Cells infected with SARS-Cov-2 and labeled with F(ab')$_2$-FITC, and observed with 20x objective. **(C)** Control infected cells incubated in the absence of F(ab')$_2$-FITC. **(D)** Control infected cells incubated in the presence of non-labeled F(ab')$_2$. First column shows images in the blue channel corresponding to Hoechst labeling of cell nuclei, second column shows images obtained in the green channel for the detection of F(ab')$_2$-FITC fluorescence, and third column is a merge of blue and green channels. Bars on (A) 100 μm, on all other images 200 μm.

Table S1 – Mean R_h values corresponding to the mean hydrodynamic radius of $F(ab')_2$ (related to Figures 3C and 4). The hydrodynamic radius (Rh) of $F(ab')_2$ samples were determined by Dynamic Light Scattering with a 630-nm laser at 25°C.

Sample	Hydrodynamic Radius, R_h nm
Anti-SARS-CoV-2 $F(ab')_2$	10.6 +/- 0.13
Antivenom $F(ab')_2$	11.8 +/- 0.21
Anti-rabies $F(ab')_2$	12,4 +/- 0.23